ISBN: 978-3-95450-227-1 ISSN: 2673-5490 doi:10.18429/JACoW-IPAC2022-TUPOTK006

SYSTEMATIC INVESTIGATION OF FLUX TRAPPING DYNAMICS IN NIOBIUM SAMPLES

F. Kramer*, S. Keckert, O. Kugeler, J. Knobloch[1], Helmholtz-Zentrum Berlin, Berlin, Germany
[1]also at Universität Siegen, Siegen, Germany

Abstract

Trapped magnetic flux in superconducting cavities can significantly increase surface resistance, and, thereby, limits the cavities' performance. To reduce trapped flux in cavities, a better understanding of the fundamental mechanism of flux trapping is vital. We develop a new experimental design: measuring magnetic flux density at 15 points just above a niobium sheet of dimensions (100 x 60 x 3) mm with a time resolution of up to 2 ms and a flux resolution better than 0.5 µT. This setup allows us to control the temperature gradient and cooldown rate, both independently of each other, as well as the magnitude and direction of an external magnetic field. We present data gathered on a large-grain sample as well as on a fine-grain sample. Our data suggests that not only the temperature gradient but also the cooldown rate affects trapped flux. Additionally, we detect a non-trivial relationship between trapped flux and magnitude of applied field.

INTRODUCTION

Rising demands on modern accelerators can in many cases only be met with superconducting cavities. This is especially true of accelerators intended to operate in continuous wave (CW) mode. Nonetheless, when operating superconducting cavities in the radio frequency (RF) range losses occur. These losses stem from non-vanishing surface resistance of superconductors in RF fields. A significant part of the surface resistance is caused by trapped flux: A perfect superconductor expels all magnetic flux when it transitions from normal conductivity to superconductivity. In contrast, real-life superconductors are not perfect, they trap magnetic flux lines. These lines oscillate in an RF field generating losses [1]. Since these cavities are operated at a temperature around 2 K, and 1 W of dissipated power requires close to 1 kW of wall plug power, the cryoplants needed to cool these cavities are a major cost driver for SRF accelerators, which is why reducing surface resistance is crucial. This permits the construction of larger machines, and reduces costs of smaller ones.

The approach to reducing trapped flux presented in this paper is to get a better understanding of the fundamental mechanism of flux trapping before trying to minimize it. To this end, we have built an experiment to measure trapped flux in samples instead of cavities [2]. This allows us to independently control the parameters which might have an influence on trapped flux (temperature gradient, cooldown rate, magnetic field). It also increases the number of possible thermal cycles drastically (~300/day instead of ~1/day). Since the samples are large flat sheets, the geometric effects that arise from demagnetisation are readily separated from effects due to the material's properties. .

First, the setup will be presented in more detail. Then, experimental data will be presented, where the parameters mentioned above (temperature gradient, cooldown rate, magnetic field) are investigated.

EXPERIMENTAL SETUP

Trapped flux in the SRF context is typically investigated using cavities [3–6]. However, experiments with cavities are costly and time consuming. Most importantly, the cavity's geometry complicates the control of cooldown parameters. It also affects how flux is trapped [7, 8]. The new setup remedies these problems:

The sample is a flat sheet of dimensions (100 x 60 x 3) mm. It is carefully clamped in between two copper blocks at the top, and bottom (Fig. 1a). These blocks can be heated with two independent heaters. Purpose of the blocks is to have the electric heaters as far away from the sample as feasible, so magnetic field created by the heaters does not reach the sample. The temperature of the sample is monitored with up to eight Cernox sensors that are glued directly on the sample (not shown in Fig. 1a). On the back side of the sample a PCB with 15 AMR sensor [9] groups is mounted barely touching the sample. In each group, three AMR single axis sensors are combined to measure the full magnetic field vector. To measure the trapped flux as closely to the sample as possible the PCB is designed such that the center of the sensor groups have a distance of only 2.3 mm to the sample. All AMR sensors are calibrated to three Fluxgate sensors. The horizontal component of the magnetic field is controlled with two Helmholtz-coils, and the vertical component is created with a solenoid wrapped around the cryostat (Fig. 1b). Since the cryostat is not shielded the earth magnetic field is compensated with the coils as well.

The magnetic field sensors can be recorded with a time resolution of up to 2 ms with a multi-channel readout system [10]. This allows us to record the dynamics during the cooldown with a very high resolution. The Cernox sensors are wired in a way that allows us to record them with this system as well. This reduces the minimal readout time from 500 ms (Lake Shore [11]), to 10 ms (reducing the readout time further creates a lot of noise). This is vital for fast cooldowns (< 1 s).

Measurement Procedure

The setup is cooled with helium gas. To achieve this the setup is mounted above a liquid helium bath. By evaporating

* f.kramer@helmholtz-berlin.de

ISBN: 978-3-95450-227-1 ISSN: 2673-5490 doi:10.18429/JACoW-IPAC2022-TUPOTK006

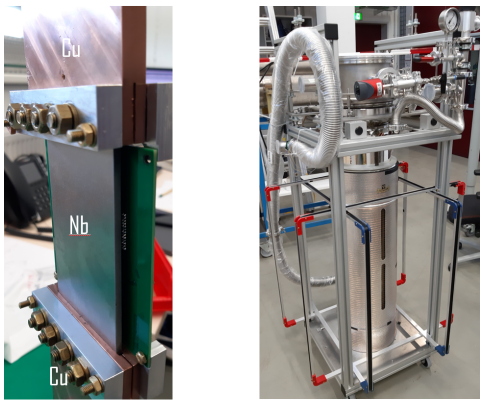

(a) Experiment (b) Cryostat

Figure 1: Picture of experimental setup. Niobium sample with copper blocks, and PCB on the left, and cryostat with Helmholtz-coils, and solenoid on the right.

helium with a heater cold gas rises, and cools down the experiment. By adjusting the heater power, gas flow can be controlled. The sample is then heated above T_c with two independently PID controlled heaters via the copper blocks. By setting different temperatures at the top and bottom of the sample, a temperature gradient is achieved. The gradient is kept constant during cooldown by lowering the set temperatures to both heaters simultaneously. The rate at which the set temperature is lowered controls the cooldown speed and can be independently regulated.

While the sample is still normal conducting the earth's magnetic field is compensated and the coil currents that are required for this are noted down. Then, a magnetic field is applied and the sample's temperature is lowered until it is fully superconducting. After it is superconducting the saved coil currents for the earth's field compensation are applied. The magnetic field measured at this time is the trapped flux in the sample.

RESULTS

Results presented in this section were recorded at two samples. Most of the presented data was recorded with a large-grain sample consisting of only two crystals with the grain boundary running horizontally through the middle of the sample. The other sample is a fine-grain sample. Both samples are cut out of cavity grade Niobium (RRR = 300). The samples are directly cut out from an untreated sheet and were not treated chemically subsequently.

To give an impression of the data taken with this setup a 3D representation of the magnetic field data is shown in Figs. 2a and 2b. In both figures a flux density of 100 µT was applied perpendicular to the sample's surface. In Fig. 2a the sample is only partially superconducting. The colors give an approximation of the position of the transition area between normal- and superconducting (from here on called "phase-front"). The position is only guessed by the magnetic field data and not based on temperature data. Above the phase-front magnetic field can pass through the sample, whereas, below it the field gets pushed around it. This also results in an increased magnetic field above the phasefront (130 µT in the second row from the top instead of 100 µT of the applied field).

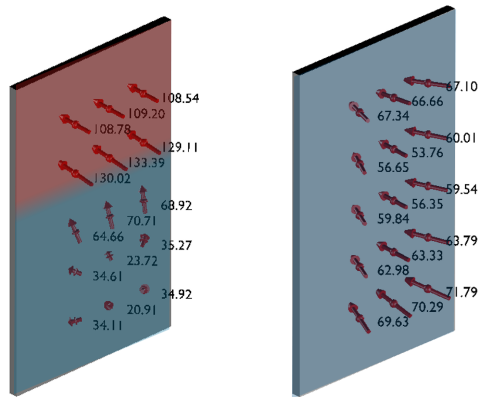

(a) Partially sc (b) Fully sc

Figure 2: 3D representation of the measured field at the 15 sensor positions. On the left the sample is only partially superconducting. On the right it is fully superconducting and the earth's magnetic field is compensated. Therefore, the measured flux stems from trapped flux in the sample.

In Fig. 2b trapped flux in a fully superconducting sample is depicted.

Trapped Flux v. Temperature Gradient

In the following, measurement results investigating the dependency of trapped flux on temperature gradient is shown. To record this data a magnetic flux density of 100 µT was applied perpendicular to the sample's surface and the cooldown rate was set to 0.07 K/s. For each cooldown a different temperature gradient was set. After the sample was fully superconducting the trapped flux was measured. In Fig.3 the resulting trapped flux is depicted for both the large-grain as well as the fine-grain. All trapped flux data in the following figures is measured in the middle row of the AMR sensor groups.

There is a striking difference between fine-grain and large-grain: For temperature gradients larger than 0.15 K/cm the large-grain sample expels all flux, whereas, the fine-grain sample never traps less than (54 ± 2) µT.

The model proposed by Kubo [12] (black fit) does not the fit the recorded data. This might be caused by the fact that the proposed model is only valid at small fields and the 100 µT at which this data was recorded does not fulfil this assumption. This data might, therefore, be valuable to extend the model. A function that fits the data well is $\exp(-\nabla T^2)$ (red fit) but there is no theory developed yet to motivate this fit.

Trapped Flux v. Ambient Field

In this section trapped flux is investigated in dependency of the flux density of the applied field. Now, the temperature

ISBN: 978-3-95450-227-1 ISSN: 2673-5490 doi:10.18429/JACoW-IPAC2022-TUPOTK006

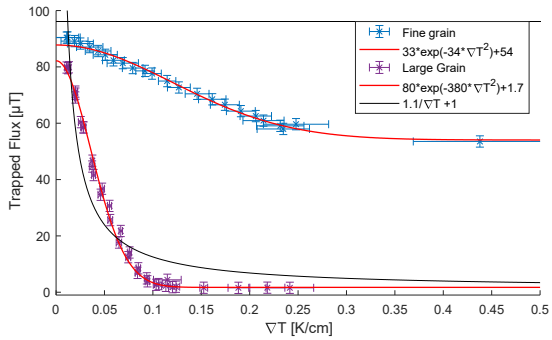

Figure 3: Trapped flux in row 3 versus temperature gradient across the sample for both large- and fine-grain. Because of the distance from the sensors to the sample, 100 µT trapped flux in the sample results only in 96 µT measured by the sensors, this is indicated in the plot with a black line.

gradient was fixed for each measurement series. During a series the magnetic flux density was then changed in 20 µT steps from −180 µT to 200 µT for each cooldown. Several series were recorded for different temperature gradients. In all series the cooldown rate was fixed at 0.07 K/s. Figure 4 shows the results.

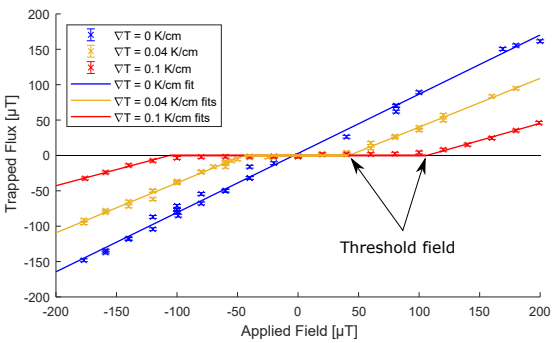

Figure 4: Trapped flux in the middle row versus the magnitude of applied flux density.

The most prominent feature is that flux is only trapped above a threshold field. The threshold field increases with increasing temperature gradient and for no temperature gradient (blue) it is zero. Once the threshold is reached the dependency on the magnetic field strength seems to be linear and the slope of the line is decreasing with increasing temperature gradient.

Trapped Flux v. Cooldown Speed

To examine how trapped flux is influenced by cooldown speed a flux density of 100 µT is applied perpendicular to the sample's surface and the temperature gradient is kept constant during a measurement series. The cooldown rate is then varied between 0.01 K/s and 2.3 K/s. The results are shown in Fig. 5

The transition time denotes the time it takes the sample to become completely superconducting once it starts at the bottom. With the logarithmic x-axis the dependency becomes very clear: Trapped flux increases with decreasing transition time. At least this is true for transition times below roughly 10 s, above that trapped flux seems to be independent of cooldown speed. This hints at a viscous force keeping the flux lines in the superconductor. This also means that "fast" cooldowns for cavities are good because they create a large temperature gradient, but if they are to fast trapped flux might actually be increased due to the speed.

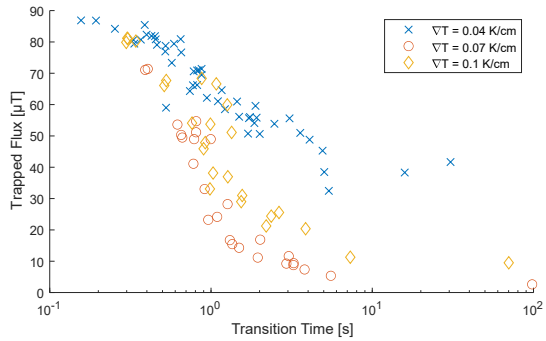

Figure 5: Trapped flux in the middle row versus transition time. "Transition time" is time it takes the sample to become completely superconducting once it starts at the bottom.

Additionally we see again that larger temperature gradients have the potential to expel significantly more flux.

It should be noted that the data is very noisy. This is due to fact that cooldowns are harder to control the faster the cooldown speed. Therefore, the temperature gradient can very between data points and the cooldown speed might change slightly during a cooldown.

CONCLUSION AND OUTLOOK

The experiments with samples confirmed existing findings, that larger temperature gradients decrease trapped flux [3], and that large-grain traps less flux than fine-grain [13]. But since the samples are cycled much quicker than cavities the curves are recorded with a high resolution. Since the data can be easily be recorded at different field levels this experiment might be used to extend the theory developed by Kubo.

In addition to that, the recorded data shows how flux only gets trapped when the external field exceeds a certain threshold field and how too fast cooldowns lead to more trapped flux.

For future measurements it is planned to perform surface and heat treatments on the samples. Additionally, we plan to test coated samples. With the help of this data it is planned to develop a phenomenological model that describes flux trapping.

REFERENCES

[1] A. Gurevich and G. Ciovati, "Effect of vortex hotspots on the radio-frequency surface resistance of superconductors,"

ISBN: 978-3-95450-227-1 ISSN: 2673-5490 doi:10.18429/JACoW-IPAC2022-TUPOTK006

Phys. Rev. B: Condens. Matter, vol. 87, no. 5, 2013, doi:10.1103/PhysRevB.87.054502

[2] F. Kramer, S. Keckert, J. Knobloch, and O. Kugeler, "Measuring flux trapping using flat samples," in *Proc. SRF'21*, East Lansing, MI, USA, 2022, paper MOPFDV003, pp. 326–330, doi:10.18429/JACoW-SRF2021-MOPFDV003

[3] A. Romanenko, A. Grassellino, A. C. Crawford, D. A. Sergatskov, and O. Melnychuk, "Ultra-high quality factors in superconducting niobium cavities in ambient magnetic fields up to 190 mG," *Appl. Phys. Lett.*, vol. 105, no. 23, p. 234 103, 2014, doi:10.1063/1.4903808

[4] D. Gonnella and M. Liepe, "Cool down and flux trapping studies on SRF cavities," in *Proc. LINAC'14*, Geneva, Switzerland, Aug.-Sep. 2014, pp. 84–87, https://jacow.org/LINAC2014/papers/MOPP017.pdf

[5] S. Huang, T. Kubo, and R. L. Geng, "Dependence of trapped-flux-induced surface resistance of a large-grain nb superconducting radio-frequency cavity on spatial temperature gradient during cooldown through tc," *Phys. Rev. Accel. Beams*, vol. 19, no. 8, p. 082 001, 2016, doi:10.1103/PhysRevAccelBeams.19.082001

[6] J. W. et al., "Development of a new b-mapping system for SRF cavity vertical tests," in *Proc. SRF'21*, East Lansing, MI, USA, 2022, paper SUPTEV009, pp. 137–141, doi:10.18429/JACoW-SRF2021-SUPTEV009

[7] D. Longuevergne and A. Miyazaki, "Impact of geometry on the magnetic flux trapping of superconducting accelerating cavities," *Phys. Rev. Accel. Beams*, vol. 24, no. 8, p. 083 101, 2021, doi:10.1103/PhysRevAccelBeams.24.083101

[8] F. Kramer, O. Kugeler, J.-M. Köszegi, and J. Knobloch, "Impact of geometry on flux trapping and the related surface resistance in a superconducting cavity," *Phys. Rev. Accel. Beams*, vol. 23, no. 12, p. 123 101, 2020, doi:10.1103/PhysRevAccelBeams.23.123101

[9] Sensitec GmbH, *AFF755B magnetoresistive field sensor*, 2022, https://www.sensitec.com/fileadmin/sensitec/Service_and_Support/Downloads/Data_Sheets/AFF700_800/SENSITEC_AFF755B_DSE_06.pdf

[10] imc Test & Measurement GmbH, *Imc spartan*, 2022, https://www.imc-tm.com/products/daq-systems/imc-spartan/overview/

[11] Lake Shore Cryotronics, *Model 218 temperature monitor*, 2022, https://www.lakeshore.com/products/categories/overview/temperature-products/cryogenic-temperature-monitors/model-218-temperature-monitor

[12] T. Kubo, "Flux trapping in superconducting accelerating cavities during cooling down with a spatial temperature gradient," *Prog. Theor. Exp. Phys.*, vol. 2016, no. 5, 053G01, 2016, doi:10.1093/ptep/ptw049

[13] S. Aull, O. Kugeler, and J. Knobloch, "Trapped magnetic flux in superconducting niobium samples," *Phys. Rev. Accel. Beams*, vol. 15, no. 6, p. 062 001, 2012, doi:10.1103/PhysRevSTAB.15.062001